



Calculation of Pile Bearing Capacity Under the Influence of Soil Cavities Based on the GM (1,3) Model

Xiaona Sun^{1*}, Dongyang Lv² and Lijun Bi¹

¹ Sichuan Polytechnic University, Deyang, Sichuan 618000, China

² Sichuan Tianyi College, Deyang, Sichuan 618200, China

*Corresponding author's e-mail: quliang0112@126.com

Abstract. This study establishes a pile-soil cavity-geotechnical model. The reliability of simulation parameters is verified through experimental piles, and load-settlement curves of piles under varying height-to-length ratios and burial depths of soil cavities are provided. The bearing capacity of piles under different conditions is analyzed. Utilizing the GM (1,3) theoretical model, a calculation formula for pile bearing capacity influenced by soil cavities is derived. The results indicate that an increase in the height-to-length ratio leads to a reduction in pile bearing capacity, with an accelerating rate of reduction. When it increases to 0.32, the pile bearing capacity decreases by 17.02%. Similarly, an increase in the burial depth of soil cavities reduces the pile bearing capacity, with a reduction of 11.80%. The impact is less significant than that of the height-to-length ratio. A formula is established to calculate the pile bearing capacity under the influence of these two factors based on the GM (1,3) theory. A comparison between theoretical calculations and simulation results shows a posterior error ratio of 0.067 and a small error probability of 1, demonstrating high calculation accuracy. The formula can be used to calculate the bearing capacity of piles under the influence of soil cavity factors. The research findings provide a theoretical reference for calculating the bearing capacity of similar engineering piles.

Keywords: geotechnical engineering, pile, cavity, bearing capacity, numerical simulation, grey theory

1 Introduction

With the development of highway, an increasing number of bridges are being built in areas with soil cavities. The soil cavities result in a loss of interaction medium for piles, and factors such as cavity height and span significantly affect the bearing of piles^[1-3]. It's difficult to determine the bearing capacity and potentially jeopardizing engineering safety^[4-5]. Therefore, it is essential to develop methods for calculating the bearing capacity of piles under the influence of soil cavities.

Currently, some researchers have investigated methods for calculating the bearing capacity of bridge piles passing through cavities^[6-7] Yao^[8] used finite element analysis

to study the characteristics of pile horizontal displacement and settlement under different relative positions between the soil cavity and pile. Chen et al.^[9-10] considering cavity erosion during the full life cycle, established bearing capacity calculation formulas using three methods. The formulas were validated against test pile design values. Liu et al.^[11] conducted laboratory model tests to study the effect of varying top plate thicknesses in karst regions on the ultimate bearing capacity of piles but did not consider the influence of cavity dimensions. Huang et al.^[12] based on field static load tests, analyzed the bearing characteristics of piles in karst regions without examining the impact of varying cavity dimensions on these characteristics. The static load tests cannot be conducted to pile failure, and the data is very scarce^[13-15]. Xia et al.^[16] employed grey system theory to establish a grey Verhulst prediction model, studying grey prediction methods for the ultimate bearing capacity of single piles in soft clay regions. Wang et al.^[17] used the GM (1,1) grey theory to predict the load-settlement relationship of bored piles and derived the bearing capacity with high prediction accuracy. Deng et al.^[18] employed multiple prediction methods for pile ultimate bearing capacity and concluded that grey prediction models have high accuracy. Cao et al. and Jia et al.^[19-20] applied an improved variable-step grey theory model to study pile bearing capacity prediction problems, proposing corresponding prediction formulas and methods. Previous studies indicate that grey theory is suitable for predicting pile bearing capacity in complex geological conditions involving both known and unknown information^[21-23].

This study employs finite element analysis to establish a pile-soil cavity-geotechnical interaction model, verifying the reliability of the model parameters. The effects of shallow soil cavity height-to-length ratios and burial depths on pile bearing capacity are investigated. A high-precision calculation method for pile bearing capacity in soil cavity regions is derived using the GM (1,3) model. The accuracy is verified by comparing theoretical values with simulation results.

2 Analysis of Pile Bearing Capacity Under the Influence of Soil Cavities

2.1 Model Development and Parameter Selection

2.1.1 Model Development.

3D model of the soil cavity-pile-geotechnic interaction is established using the Midas GTS NX software. The dimensions of the geotechnic in the X and Y directions are 60 m, and Z direction is 70 m. The model cross-section is shown in Figure 1. The geotechnical body is modeled with an elastic-plastic constitutive model, satisfying the Mohr-Coulomb yield criterion. The pile-soil contact interface is simulated using Goodman elements, and the cavity is modeled as a void, ignoring any filling material. The pile is represented as a 3D cylindrical model made of concrete, with an ideal elastic constitutive model. The pile diameter is 1.5 m. The bottom boundary is constrained in the X, Y, and Z directions; The lateral boundaries are constrained in the X and Y directions; The upper surface is a free boundary.

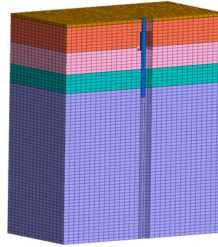


Fig. 1. Model.

2.2.2 Parameters and Conditions.

The parameters of materials are listed in Table 1.

Table 1. Physical and Mechanical Parameters of Materials.

Name	Elastic modulus E_s/MPa	Unit weight $\gamma/(\text{kN}\cdot\text{m}^{-3})$	Cohesion c/kPa	Friction angle $\phi/^\circ$	Poisson ratio μ	Depth /m
①	25.0	18.0	5.0	10.0	0.35	1.0
②	45.0	17.0	13.2	29.5	0.30	7.8
③	60.0	18.0	10.8	33.5	0.28	6.7
④	300.0	24.0	150.0	30.0	0.25	6.0
⑤	1000.0	26.0	200.0	38.0	0.22	3.5
pile	3×10^{10}	25.0	/	/	0.20	25.0

The geology of the SZ pile is shown in Figure 2. The pile has a diameter of 1.5 m, a length of 25.0 m, and an embedment depth of 3.5 m. It is made of C30 concrete, with a height-to-length ratio of 0.16 and a burial depth of 2.0 m. The field test applies graded loading corresponding to each construction stage of the superstructure. Working conditions 1 to 5 represent the self-weight of the pier, tie beam, cap beam, box girder, and bridge deck, respectively. The loads are 320 kN, 1120 kN, 2150 kN, 3258 kN, 4039 kN. The pile settlement measurement point is shown in Figure 3.

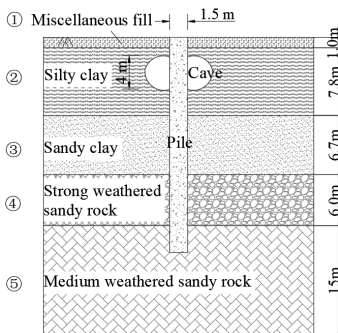


Fig. 2. Geological Conditions.

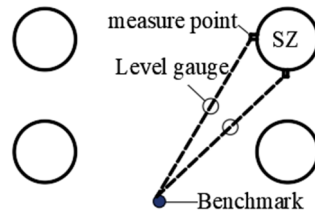


Fig. 3. Layout of Measurement Points.

A simulation model is established using the SZ pile as a prototype to verify the reliability of the finite element numerical model and its constitutive relationships. Since the self-weight loads of the pier, tie beam, cap beam, box girder, bridge deck, and crash barriers are relatively small, the pile settlement measured under graded loading of the field test is also minor. A comparison between the simulation results and the field test results is shown in Figure 4.

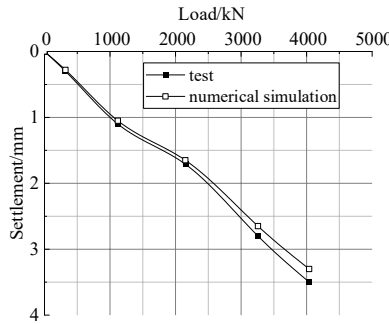


Fig. 4. Comparison of Load-Settlement Curves.

As shown in Figure 4, the slope of the load-settlement curve obtained from the numerical simulation is slightly smaller than that of the field test results. Under the same load, the settlement of the pile in the numerical simulation is smaller. The main reason is that the numerical simulation model is more idealized, and the side resistance generated by the pile-soil -cavity interaction is larger. Under the effect of construction loads, the load-settlement curve obtained from the numerical simulation shows a trend that is generally consistent with the field test results. The numerical simulation model can be used to study the impact of different soil cavity parameters on the bearing characteristics of pile foundations.

2.1.3 Working Condition Design.

Using the soil cavity height-to-span ratio and burial depth as variables, different numerical simulation models are established. Existing research indicates that the height of the cavity has a greater impact on the pile, while the span has less effect. In the simulations, it is assumed that the span in the X and Y directions is the same, set to 2 m, and the height is varied to change the height-to-span ratio. The design scheme is shown in Table 2, where A represents the ratio of soil cavity height to pile length, referred to as the height-to-length ratio.

Table 2. Scheme Design.

Height-to-Length Ratio A/m	Buried Depth Z/m
0.04, 0.08, 0.16, 0.24, 0.32	2, 4, 6, 8, 10

2.2 Analysis of Bearing Capacity Calculation Results

2.2.1 Analysis of Pile Bearing Capacity under Varying Height-to-Length Ratios.

The load-settlement (Q - s) curves of the pile under the influence of soil cavity are shown in Figure 5, and the variations in pile bearing capacity are depicted in Figure 6.

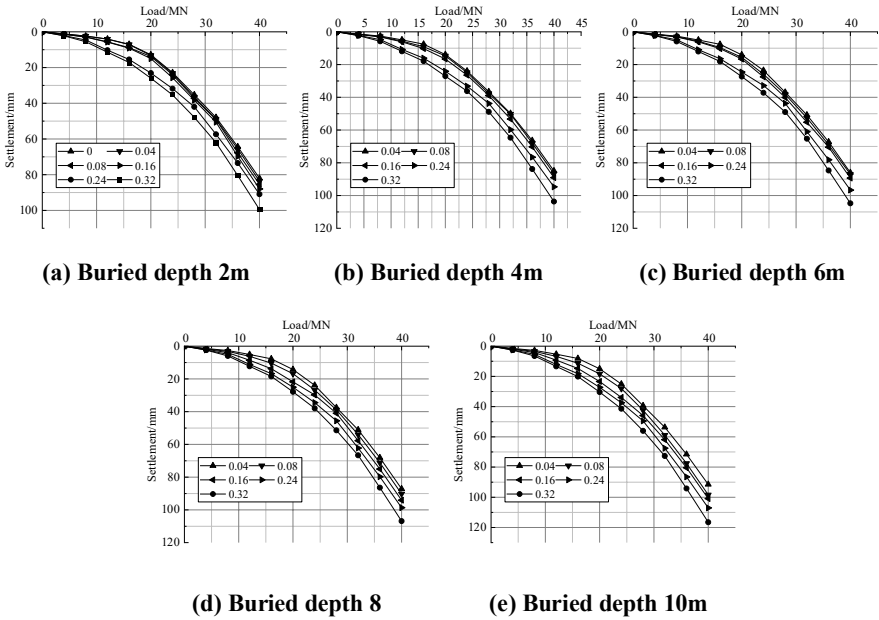


Fig. 5. Q-s Curve under Height-to-Length Ratios.

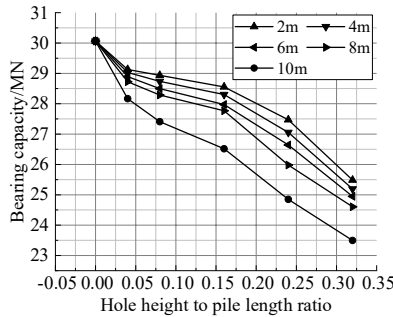


Fig. 6. Pile Bearing Capacity under the Influence of Height-to-Length Ratios.

As observed in Figure 5 and 6, compared to the case without a soil cavity, the presence of a cavity increases the settlement of the pile top under the same load and decreases the pile's bearing capacity. As A (the height-to-length ratio) increases, the load required to produce the same settlement at the pile top decreases, leading to a gradual reduction in pile bearing capacity, with an increasing rate of reduction. Taking a burial depth of 6 m as an example, as A increases from 0 to 0.32, the reduction in pile bearing

capacity is 3.90%, 5.21%, 6.95%, 11.38%, and 17.02%, respectively. This indicates that as the height of the soil cavity increases, A increases, resulting in a reduction of the soil surrounding the pile foundation. Consequently, the medium compressing the pile foundation decreases, the side resistance of the pile becomes discontinuous, and the reduction in pile bearing capacity intensifies.

2.2.2 Analysis of Pile Bearing Capacity under Varying Burial Depths.

The load-settlement (Q - s) curves of the pile under the influence of soil cavity are shown in Figure 7, and the variations in pile bearing capacity are depicted in Figure 8.

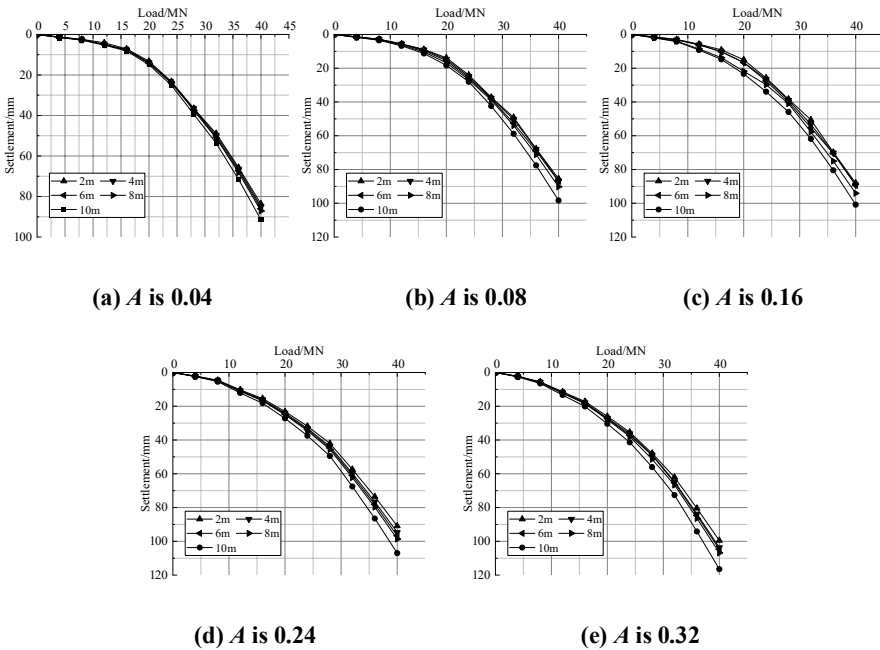


Fig. 7. Q-s Curve under the Influence of Soil Cavity Burial Depth.

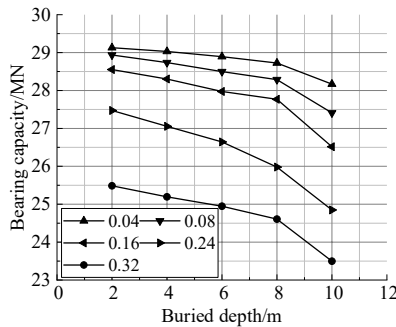


Fig. 8. Pile Bearing Capacity under the Influence of Soil Cavity Burial Depth.

As observed in Figure 7 and 8, increasing the burial depth of the soil cavity reduces the load required to produce the same settlement at the pile top, leading to a gradual reduction in pile bearing capacity, with an increasing rate of reduction. Taking $A=0.16$ as an example, as the burial depth of the soil cavity increases from no cavity to 10 m, the influence on pile bearing capacity is 5.03%, 5.86%, 6.95%, 7.64%, and 11.80%, respectively. Although the impact of increasing burial depth on pile bearing capacity becomes more significant, it remains less influential compared to the effect of the height-to-length ratio. The primary reason is that as depth increases, the standard value of lateral resistance in the soil layer also increases. For the same height-to-length ratio of the soil cavity, the pile's lateral resistance is more effectively utilized. However, increasing burial depth causes a greater loss of lateral resistance.

3 GM (1,3) Model

3.1 Establishment of the Grey GM (1,3) Model

The grey model theory is applied to construct a model considering the influences of height-to-length ratio and burial depth. The model includes three variables: the pile bearing capacity (Q_j), the height-to-length ratio (A), and the burial depth (Z). A GM (1,3) model^[24] is established to derive the relationship between the bearing capacity under soil cavity conditions and the height-to-length ratio and burial depth.

The initial data in the GM (1,3) model are:

$$\begin{cases} Q_j^{(0)} = [Q_j^{(0)}(1), Q_j^{(0)}(2), \dots, Q_j^{(0)}(25)] \\ A^{(0)} = [A^{(0)}(1), A^{(0)}(2), \dots, A^{(0)}(25)] \\ Z^{(0)} = [Z^{(0)}(1), Z^{(0)}(2), \dots, Z^{(0)}(25)] \end{cases} \tag{1}$$

The first-order accumulated data in the GM (1,3) model are:

$$\begin{cases} Q_j^{(1)} = [Q_j^{(1)}(1), Q_j^{(1)}(2), \dots, Q_j^{(1)}(25)] \\ A^{(1)} = [A^{(1)}(1), A^{(1)}(2), \dots, A^{(1)}(25)] \\ Z^{(1)} = [Z^{(1)}(1), Z^{(1)}(2), \dots, Z^{(1)}(25)] \end{cases} \tag{2}$$

in which:

$$Q_j^{(1)}(k) = \sum_{i=1}^k Q_j^{(0)}(i), \quad A^{(1)}(k) = \sum_{i=1}^k A^{(0)}(i), \quad Z^{(1)}(k) = \sum_{i=1}^k Z^{(0)}(i) \tag{3}$$

Where: $k = 1, 2, 3, \dots, 25$.

The initial sequences of Q_j , A , and Z are shown in Figure 6 and 8. To ensure the original data exhibit an overall increasing trend and effectively reduce errors, a value of 40 is uniformly subtracted from the bearing capacity. This adjustment produces the

original data for the three variables, as shown in Figure 9. Using Equation(2) , the first-order accumulated sequence is obtained, as shown in Figure 10.

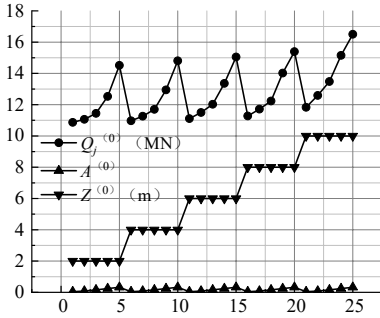


Fig. 9. Original Data Chart.

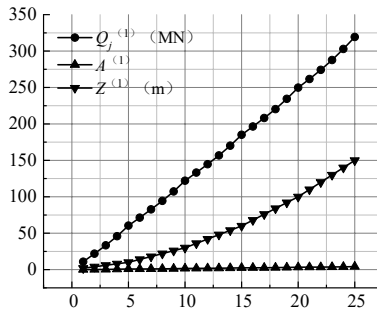


Fig. 10. 1-AGO Data.

Based on grey system theory, the whitening differential equation is established as follows:

$$\frac{dQ_j^{(1)}}{dt} + aQ_j^{(1)} = b_1A^{(1)} + b_2Z^{(1)} \tag{4}$$

where: a —development coefficient(1/mm), b_1, b_2 —grey effect(kN/mm).

The value of \hat{a} can be calculated using the least squares method, that is:

$$\hat{a} = (B^T B)^{-1} B^T y_n \tag{5}$$

Where:

$$B = \begin{bmatrix} -\frac{1}{2}(Q_j^{(1)}(1)+Q_j^{(1)}(2)) & A^{(1)}(2) & Z^{(1)}(2) \\ -\frac{1}{2}(Q_j^{(1)}(2)+Q_j^{(1)}(3)) & A^{(1)}(3) & Z^{(1)}(3) \\ \vdots & \vdots & \vdots \\ -\frac{1}{2}(Q_j^{(1)}(24)+Q_j^{(1)}(25)) & A^{(1)}(25) & Z^{(1)}(25) \end{bmatrix} \tag{6}$$

$$y_n = [Q_j^{(0)}(2), Q_j^{(0)}(3), \dots, Q_j^{(0)}(25)]^T \tag{7}$$

So, $\hat{a} = [a, b_1, b_2]^T = (-0.19, 0.67, -0.33)^T$

Expanding the GM (1,3) model, we get the relationship:

$$Q_j^{(0)}(k) = \alpha_1 A^{(0)}(k) + \alpha_2 Z^{(0)}(k) + (1 - \eta) Q_j^{(0)}(k - 1) \tag{8}$$

where, $\alpha_1 = \frac{b_1}{1+0.5a}, \alpha_2 = \frac{b_2}{1+0.5a}, \eta = \frac{a}{1+0.5a}$

By performing parameter calculations and restoring the initial data, the formula for calculating the pile bearing capacity under the influence of soil cavities is derived:

$$Q_j^{(0)}(k) = 40 - 0.74A^{(0)}(k) + 0.36Z^{(0)}(k) - 1.21Q_j^{(0)}(k-1) \quad (9)$$

3.2 Verify the Reliability of the Formula

Substituting A and Z for each working condition, the corresponding pile bearing capacity is calculated and compared with the simulation results, as shown in Figure 11.

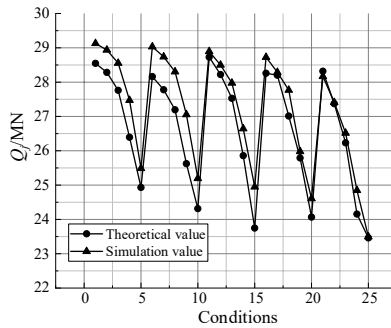


Fig. 11. Comparison of Predicted and Theoretical Values.

As shown in Figure 11, the bearing capacity calculated using the formula derived from the GM (1,3) theoretical model has a maximum relative error of 5.29% compared to the simulation results, with an average residual error of 2.69%. According to the accuracy evaluation criteria of grey theory, the calculated posterior error ratio is 0.067, and the small error probability is 1, indicating that the calculation accuracy of the bearing capacity is rated as "good."

4 Conclusion

(1) The pile bearing capacity shows a negative correlation with the soil cavity height-to-length ratio and burial depth. As the height-to-length ratio increases, the pile bearing capacity decreases at an accelerating rate. When the height-to-length ratio increases to 0.32, the bearing capacity decreases by 17.02%. Within the burial depth range of 2–10 m, the pile bearing capacity decreases as the burial depth increases. When the burial depth reaches 10 m, the bearing capacity decreases by 11.80%. The impact of the height-to-length ratio on pile bearing capacity is greater than that of the burial depth.

(2) The calculation formula for pile bearing capacity under the influence of the soil cavity height-to-length ratio and burial depth, established using the GM (1,3) model, achieves a posterior error ratio of 0.067 and a small error probability of 1, indicating high calculation accuracy. This formula can be used to calculate pile bearing capacity in geological conditions involving soil cavities.

(3) The grey GM (1, N) model is applicable for calculating pile bearing capacity under multifactor influence when on-site bearing capacity tests cannot be conducted, or data is limited. It demonstrates significant practical value in engineering applications.

References

1. Liang J H, Fan Q Y, Liu Me H and Li T Y. Physical model test on the influence of karst cave under and in front of pile on the stability of embedded end of antislid pile[J]. *Mathematical Problems in Engineering*,2022.
2. Chen H Y, Feng Z J, Xia C M. Bearing characteristic centrifugal test and bearing capacity calculation method of pile foundation passing through karst cave[J]. *Chinese Journal of Underground Space and Engineering*, 2023, 19(03) : 856-866+880.
3. Wang P, Ding H, Zhang P. Influence of karst caves at pile side on the bearing capacity of super-long pile foundation[J]. *Mathematical Problems in Engineering*, 2020, 2020(2) : 1-13.
4. CHEN H Y, FENG Z J, LI T. Study on the vertical bearing performance of pile across cave and sensitivity of three parameters. *Scientific Reports*, 2021; 11: 17342.
5. LIANG X, CHENG Q G, YANG T. Numerical simulation on mechanical mechanism of pile-group foundation of high-speed railway in goaf area[J]. *Railway Standard Design*,2014,58(05) : 49-54.
6. MEI Gu X, LU Z Y, CHEN J X. Experiment and simulation research on bearing mechanism of a new type grouted pile in karst area[J]. *Journal of Hunan University (Natural Sciences)* ,2022,49(07) : 32-44.
7. LEI Y, LI P J, LIU Z Y. Calculation method and experimental study on the critical load of buckling for foundation piles crossing karst caves in karst areas. *Rock and Soil Mechanics*, 2022 (12) : 1-10.
8. YAO Y J. Study on the impact of soil caves on the stability of foundation pits in karst areas. Master' s Thesis, Guilin University of Technology, 2020.
9. CHEN H Y, FENG Z J, XIE F G. Study on the calculation method for the rock embedding depth of foundation piles crossing karst caves in bridge engineering. *Bridge Construction*, 2024, 54(03) : 109-116.
10. CHEN H Y, FENG Z J, XIA C M. Centrifugal test and bearing capacity calculation method for foundation piles in karst caves. *Underground Space and Engineering Journal*, 2023, 19(03) : 856-866+880.
11. Liu L, Shi Z M, Tsoflias G P, Peng M and Wang Y. Detection of karst voids at pile foundation by full-waveform inversion of single borehole sonic data[J]. *Soil Dynamics and Earthquake Engineering*.2022.
12. HUANG S G,MEI S L,GONG W M. Testing study on bearing behavior of piles for Nan-Pan river great Bridge in karst area[J]. *Chinese Journal of Rock Mechanics and Engineering*.2004(05) : 809-813.
13. FENG H L, LIU D M, CAI G J. Evaluation method for the pullout bearing characteristics of piles based on CPTU testing. *Rock Mechanics and Engineering Journal*, 2023, 42(S1) : 3778-3791.
14. LIANG X, CHENG Q G, CHEN J M. Model test on pile group foundation of a high-speed railway bridge above a goaf[J]. *Rock and Soil Mechanics*, 2015,36(07) : 1865-1876.
15. LEI Y, YIN J F, CHEN Q N. Experimental study on ultimate bearing capacity and failure mode of pile foundation in karst area[J]. *Chinese Journal of Applied Mechanics*,2017,34(4) : 1-7.

16. XIA Ji Z, LUO Z Y, ZHANG S Z. Analysis and prediction of the time-dependent bearing capacity of compression piles in soft clay. *Rock and Soil Mechanics*, 2006, 27(S2) : 793-796.
17. WANG C H, LI W J. The grey prediction model of the load-settlement relationship for bored piles. *Building Structures*, 2004, (09) : 47-48+46.
18. DENG Z Y, LU P Y. Comparative analysis of several vertical ultimate bearing capacity prediction models for single piles. *Rock and Soil Mechanics*, 2002, (04) : 428-431+464.
19. CAO X G,ZHANG Y J,ZHAO M H. Study on application of improved gray predicted method to determining ultimate bearing capacity of single pile[J]. *Rock and Soil Mechanics*,2006,27(S2): 774-778.
20. JIA K, LIU J P, WANG M. The Settlement Prediction of Pile Foundation Based on Grey Linear Regression Model[J]. *Applied Mechanics and Materials*, 2012, 1975(204) .
21. JIANG W J,YAN D Y,WANG M M. Load-settlement rules and calculation of foundation piles in karst cave[J]. *Chinese Journal of Geotechnical Engineering*,2017,39(S2) : 67-70.
22. WANG C H,ZHANG M N. Grey theoretical modification prediction method for the load-settlement curve of bored piles. *Journal of Shenyang Jianzhu University (Natural Science Edition)* , 2013, 29(02) : 270-276.
23. YAO Y J. Study on the impact of soil caves on the stability of foundation pits in karst areas. Master's Thesis, Guilin University of Technology, 2020.
24. DENG J L. Basic methods of grey systems. Wuhan: Huazhong University of Science and Technology Press,1988,10-55.

Open Access This chapter is licensed under the terms of the Creative Commons Attribution-NonCommercial 4.0 International License (<http://creativecommons.org/licenses/by-nc/4.0/>), which permits any noncommercial use, sharing, adaptation, distribution and reproduction in any medium or format, as long as you give appropriate credit to the original author(s) and the source, provide a link to the Creative Commons license and indicate if changes were made.

The images or other third party material in this chapter are included in the chapter's Creative Commons license, unless indicated otherwise in a credit line to the material. If material is not included in the chapter's Creative Commons license and your intended use is not permitted by statutory regulation or exceeds the permitted use, you will need to obtain permission directly from the copyright holder.

